Supporting Information for

Changes in non-dipolar field structure over the Plio-Pleistocene: New paleointensity results from Hawai‘i compared to global datasets

Brendan Cych[a], Lisa Tauxe[a], Geoff Cromwell[b], John Sinton[c], and Anthony A.P. Koppers[d] 1

[a]University of California, San Diego; [b]Occidental College; [c]University of Hawai'i at Manōa; [d]Oregon State University

Brendan Cych. E-mail: bcych@ucsd.edu

This PDF file includes:

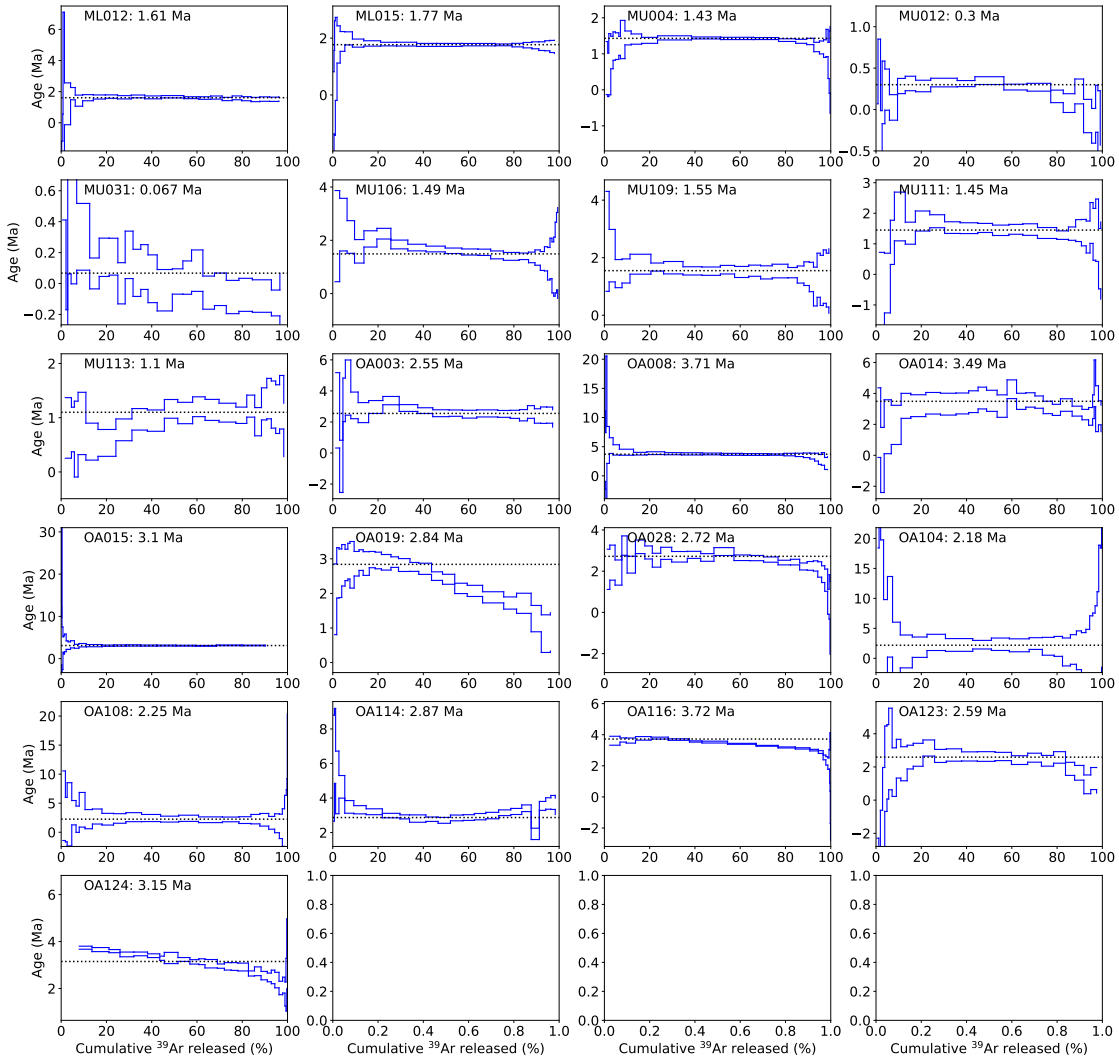

Fig. S1. Plots of Age against cumulative Argon released for age plateau and mini-plateau (OA019, OA116, OA124) age experiments. The mini-plateau ages for OA124 are concordant with total fusion ages from other samples from same site, and the mini-plateau age for OA019 is close to the age for OA028, a nearby lava flow which it is stratgraphically below.

Brendan Cych[a], Lisa Tauxe[a], Geoff Cromwell[b], John Sinton[c], and Anthony A.P. Koppers[d]

Table S1. Results analyzed using BiCEP from Antarctica (1) (sites with the prefix 'mc') and Northern Israel (2) (sites with the prefix 'GHI')

Site	Latitude	Longitude	Age (Ma)	Age 2σ	B_{min}	B_{median}	B_{max}
mc1001	-77.850000	166.640000	1.1800	0.0100	12.7	18.6	24.9
mc1002	-77.850000	166.690000	0.3300	0.0200	22.3	29.1	36.3
mc1009	-77.550000	166.200000	0.0740	0.0150	23.9	28.0	35.1
mc1015	-77.470000	169.230000	1.3300	0.0200	22.7	26.7	30.6
mc1020	-77.880000	165.020000	0.7700	0.0320	55.6	62.3	69.3
mc1029	-78.310000	164.800000	0.1800	0.0800	41.7	44.7	48.0
mc1031	-78.350000	164.300000	0.1330	0.0117	23.5	31.2	39.0
mc1032	-78.360000	164.300000	0.0078	0.0120	27.9	31.2	34.9
mc1036	-78.390000	164.270000	0.1200	0.0400	22.2	28.8	35.3
mc1103	-78.240000	163.360000	1.4210	0.0300	14.5	20.1	27.7
mc1109	-78.280000	163.540000	1.2610	0.0400	29.5	33.2	37.0
mc1111	-78.220000	162.790000	1.9900	0.0400	18.5	21.4	24.6
mc1115	-78.240000	162.960000	2.4600	0.3100	26.7	31.2	35.8
mc1119	-78.240000	162.960000	1.0800	0.2200	34.6	37.7	40.9
mc1120	-78.240000	163.090000	1.7560	0.0500	22.4	24.7	27.0
mc1121	-78.240000	162.950000	2.5050	0.0600	28.8	32.8	35.7
mc1127	-78.250000	163.730000	1.9420	0.0680	33.7	37.0	40.4
mc1135	-78.230000	166.560000	3.6000	0.0100	29.4	31.7	33.9
mc1139	-78.260000	163.080000	0.8820	0.0800	24.6	27.8	31.0
mc1140	-78.280000	163.000000	2.0430	0.0900	28.4	34.2	39.1
mc1145	-78.240000	162.893000	1.9000	0.1200	3.3	7.0	10.2
mc1147	-78.200000	162.960000	1.6300	0.3200	16.5	22.4	27.2
mc1155	-77.700000	162.250000	1.5000	0.0500	23.3	30.8	38.3
mc1157	-77.700000	162.260000	1.7100	0.0100	31.4	37.9	44.9
mc1160	-77.690000	162.350000	3.4700	0.0500	18.1	24.9	31.4
mc1165	-77.510000	169.330000	1.4510	0.0600	20.6	27.8	35.1
mc1167	-77.490000	169.290000	1.3800	0.1000	38.9	43.5	48.4
mc1200	-77.550000	166.160000	0.0730	0.0100	21.2	26.6	31.8
mc1302	-78.190000	165.320000	0.0400	0.0200	23.7	28.9	34.3
mc1304	-78.240000	163.360000	0.2900	0.0400	18.8	24.7	29.5
mc1305	-78.240000	163.230000	0.9000	0.2000	30.6	34.4	38.2
mc1306	-77.700000	162.690000	2.5600	0.2600	4.5	6.9	9.5
mc1307	-77.850000	166.670000	1.3300	0.2400	39.7	46.1	53.5
GHI01	33.126350	35.782270	0.1177	0.0358	20.1	25.2	30.2
GHI02	33.158050	35.776730	0.1296	0.0012	20.5	24.5	27.9
GHI03B	33.122790	35.724160	0.8420	0.0233	66.7	69.3	72.2
GHI03C	33.122790	35.724160	0.8420	0.0233	36.8	45.2	52.5
GHI03D	33.122790	35.724160	0.8420	0.0233	47.0	59.2	70.1
GHI05	32.960510	35.862240	0.1679	0.0255	19.7	22.6	25.0
GHI06	33.069580	35.771430	0.1145	0.0085	26.4	27.4	28.5
GHI07	33.085810	35.755890	0.6805	0.0183	33.6	40.9	47.7
GHI07C	33.085810	35.755890	0.6805	0.0183	21.0	23.2	25.2
GHI10	33.051680	35.849680	0.6149	0.0349	18.1	19.8	21.5
GHI18	33.025833	35.494912	1.6700	0.0400	30.9	37.3	43.6
GHI19	32.995278	35.525986	2.4500	0.0226	27.1	32.8	39.4
GHI20	32.926290	35.849940	1.6500	0.0200	29.9	31.8	33.5
GHI21	32.926290	35.849940	1.6765	0.0302	21.7	23.6	25.6
GHI25	33.218726	35.777062	0.8723	0.0053	44.7	52.9	60.8
GHI26	33.220000	35.776833	0.8704	0.0169	46.2	50.0	53.7
GHI27	33.212500	35.786157	1.1498	0.0348	33.5	36.9	40.6
GHI28	33.212500	35.786157	1.1912	0.0152	21.5	28.0	33.7
GHI29	33.179444	35.793218	0.7496	0.0945	28.7	31.1	33.2
GHI39	33.141000	35.682000	0.8476	0.1165	5.9	14.8	21.7
GHI40	33.141000	35.682000	0.7736	0.1949	4.7	7.1	9.8
GHI41	33.141000	35.683000	0.7902	0.0058	4.7	7.1	10.0
GHI44	33.042000	35.836000	1.4369	0.0195	45.6	48.9	52.6
GHI46	32.868290	35.829050	2.7442	0.0475	51.2	61.2	75.4

References

1. H Asefaw, L Tauxe, AAP Koppers, H Staudigel, Four-Dimensional Paleomagnetic Dataset: Plio-Pleistocene Paleodirection and Paleointensity Results From the Erebus Volcanic Province, Antarctica. *J. Geophys. Res. Solid Earth* **126**, e2020JB020834 (2021).
2. L Tauxe, H Asefaw, N Behar, AAP Koppers, R Shaar, Paleointensity Estimates from the Pleistocene of Northern Israel: Implications for hemispheric asymmetry in the time-averaged field. *Geochem. Geophys. Geosyst.* **n/a**, e2022GC010473 (2022).